ChemPubSoc Europe

DOI: 10.1002/chem.201701216

CHEMISTRY
A European Journal
Communication

Dyes/Pigments

Hydroxylated Fluorescent Dyes for Live-Cell Labeling: Synthesis, Spectra and Super-Resolution STED** Microscopy

Alexey N. Butkevich,*[a] Vladimir N. Belov,*[a] Kirill Kolmakov,[a] Viktor V. Sokolov,[b] Heydar Shojaei,[a] Sven C. Sidenstein,[a] Dirk Kamin,[a] Jessica Matthias,[c] Rifka Vlijm,[c] Johann Engelhardt,[c] and Stefan W. Hell*[a]

Abstract: Hydroxylated rhodamines, carbopyronines, silico- and germanorhodamines with absorption maxima in the range of 530–640 nm were prepared and applied in specific labeling of living cells. The direct and high-yielding entry to germa- and silaxanthones tolerates the presence of protected heteroatoms and may be considered for the syntheses of various sila- and germafluoresceins, as well as -rhodols. Application in stimulated emission depletion (STED) fluorescence microscopy revealed a resolution of 50–75 nm in one- and two-color imaging of vimentin-HaloTag fused protein and native tubulin. The established structure–property relationships allow for prediction of the spectral properties and the positions of spirolactone/zwitterion equilibria for the new analogues of rhodamines, carbo-, silico-, and germanorhodamines using simple additive schemes.

Among the multitude of fluorophores reported so far, only rhodamines,[1] carbopyronines,[1a] and silicon-rhodamines (SiR)[2] bearing a carboxyl in the *ortho*-position of the pendant aromatic ring provide specific vital labeling and perform well in super-resolution fluorescence microscopy. These dyes exist in equilibrium between zwitterionic (fluorescent) and spirolactone (non-fluorescent) forms. Many cationic lipophilic triarylmethanes bind non-specifically and stain membrane structures.[3] Numerous anionic fluorescent labels, commercially available as sulfonates or phosphates, are hydrophilic and highly water soluble but do not penetrate the plasma membrane and are therefore used nearly exclusively in immunostaining of fixed cells; alternative strategies of membrane-impermeant label delivery employ cell-penetrating peptide conjugates[4] and reversible permeabilization.[5]

On the contrary, several rhodamine-type dyes specifically stain intact cells when applied as conjugates with small molecule recognition units.[1a, 2a, c, 6] The most widely used recognition units are BG-NH_2, BC-NH_2 and HaloTag amine (covalent ligands of the SNAP-tag,[7] CLIP-tag,[8] and HaloTag proteins[9]). Several non-covalent ligands (such as docetaxel, jasplakinolide, or pepstatin A, binding to native β-tubulin,[2b] F-actin,[2b] or aspartyl proteases in lysosomes,[2c] respectively) have been successfully used as conjugates with fluorescent dyes (see Figure S1, Supporting Information). However, the affinity and staining specificity of a given marker depends on the cell line, the nature of the ligand and the dye, the length of the linker between them, and the cell staining buffer composition.[2b] Moreover, the spectral variety of photostable dyes suitable for live cell super-resolution microscopy still remains limited.

To address some of the above-stated limitations, we have recently proposed the introduction of hydroxyl groups into the fluorescent dye molecules as a method for increasing polarity, improving solubility in water and preventing unspecific binding. In our previous study, we reported the dye *580R*[1a, 10] (a live-cell two-color STED imaging marker), a rhodamine with two hydroxyl groups in allylic positions. In *580R* and its predecessor Atto 590,[1b] the conjugated alkene bonds in dihydroquinoline fragments provide the bathochromic and bathofluoric shifts.[1a, 10] However, these fragments are prone to photo-oxidation and may negatively affect the photostablity.[11] Aimed at

[a] *Dr. A. N. Butkevich, Dr. V. N. Belov, Dr. K. Kolmakov, Dr. H. Shojaei, Dr. S. C. Sidenstein, Dr. D. Kamin, Prof. Dr. Dr. S. W. Hell*
Department of Nanobiophotonics,
Max Planck Institute for Biophysical Chemistry (MPIBPC),
Am Fassberg 11, 37077 Göttingen (Germany)
E-mail: abutkev@gwdg.de
vbelov@gwdg.de
shell@gwdg.de
Homepage: http://www.mpibpc.gwdg.de/abteilungen/200/

[b] *Dr. V. V. Sokolov*
Department of Chemistry,
St. Petersburg State University, Universitetskiy Pr. 26,
198504 St. Petersburg (Russia)

[c] *J. Matthias, Dr. R. Vlijm, Dr. J. Engelhardt*
German Cancer Research Center (DKFZ),
Im Neuenheimer Feld 280, 69120 Heidelberg (Germany)

[**] *STED: stimulated emission depletion.*

Supporting information and the ORCID identification number(s) for the author(s) of this article can be found under https://doi.org/10.1002/chem.201701216.

Part of a Special Issue to celebrate the 150th anniversary of the German Chemical Society (GDCh). To view the complete issue, visit https://doi.org/chem.v23.50.

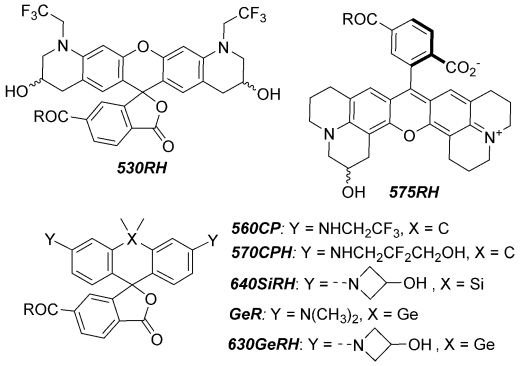

Figure 1. Membrane-permeant and fluorescent rhodamines (*R*), carbopyronines (*CP*), silico- (*SiR*) or germanorhodamines (*GeR*) designed for STED microscopy of living cells (in free dyes, R = OH; in dye-ligand conjugates, R = NH-ligand or NH-linker-ligand). *H* in names stands for hydroxylated fluorophores.

developing methods for preventing unspecific binding and improving water solubility of fluorescent dyes for living cells, we designed fluorophores with additional hydroxy groups (*530RH* and *575RH*, Figure 1) in non-allylic and non-benzylic positions.

Substitution of an oxygen atom in pyronines with a group 14 element atom (X = Si, Ge, Sn) leads to significant bathochromic shifts in the absorption and emission spectra.[2,12] The effect is due to lower LUMO energy of these fluorophores explained by conjugation between the σ* orbitals of exocyclic X–R bonds and the π*-system of the X-containing tricyclic fragment.[12] The extent of the red shift falls in the order Si > Ge > Sn (≫ C), as the efficiency of σ*–π* overlap decreases with the increasing atomic radius of X and C–X bond length. The corresponding Sn-pyronine dyes are unstable; however, *GeR* dye, the direct Ge analogue of the widely used fluorogenic dye *SiR*,[2a] and its bis-azetidinyl analogue (Ge analogue of the dye JF_{646}[6]) remain unknown[13] (Supporting Information Figure S2). To investigate the properties of the new fluorophores and the influence of hydroxylation on staining specificity, we prepared dyes listed in Table 1 (see also Figure S3 in the Supporting Information).

Bis-hydroxylated dye *530RH* with 6′-carboxy-Q-rhodamine (Rh_Q-CO_2H)[14] core was prepared according to Scheme 1a. Although the parent Rh_Q-CO_2H is cell-permeant and its conjugate with HaloTag amine provided specific staining in living cells,[1d] the dye is poorly soluble in aqueous media and its secondary amino groups are prone to acylation, which renders the NHS ester unstable. To circumvent these drawbacks, a new dye *530RH* was designed, bearing two 2,2,2-trifluoroethyl groups to block its nitrogen atoms from acylation and two hydroxyl groups to offset the hydrophobic properties of *N*-trifluoroethyl substituents. These substituents impart only slight bathochromic shifts in the absorption and emission spectra, but shift the equilibrium between the zwitterionic and spirolactone forms significantly towards the latter,[1a] facilitating cell membrane penetration. Following the same logic, the dye *560CP* (Supporting Information Figure S4) and its hydroxylated analogue *570CPH* were designed as useful derivatives of the *N*,*N*′-unsubstituted carbopyronine, which itself has not yet found any application in fluorescent labeling.

Table 1. Spectral properties of cell-permeant dyes in aqueous PBS buffer (pH 7.4) at room temperature (STED at 775 nm, unless noted otherwise).

Dye	Absorption λ_{max}, nm (ε, M^{-1} cm^{-1})	Emission λ_{max}, nm (Φ_{fl})[a]	Brightness rel. to *SiR*[b]	$D_{0.5}$[c]	Fluor. lifetime τ, ns
Rh_QCO_2H[1d]	540 (70 000)	561 (0.79)	1.45	< 5.6	4.0
530RH	532 (56 000)	553 (0.89)[d,e]	1.31	29.6	4.0
560CP	561 (61 000)	588 (0.76)[e]	1.22	71.0	4.2
570CPH	571 (79 000)	600 (0.71)	1.47	58.5	4.0
6-ROX[f]	575 (82 000)	602 (0.76)	1.63	< 5.6	4.3
575RH	574 (55 000)	597 (0.74)	1.07	< 5.6	4.3
GeR	634 (97 000)	655 (0.43)	1.09	65.2	2.7
630GeRH	631 (61 000)	651 (0.60)	0.96	72.2	3.2
SiR[2]	645 (93 000)	661 (0.41)	1 (ref.)	64.5	2.7
640SiRH	641 (51 000)	662 (0.42)	0.56	72.4	3.2

H denotes hydroxylated fluorophores. [a] absolute values; [b] relative brightness expressed as $(\varepsilon \times \Phi_{fl})_{dye}/(\varepsilon \times \Phi_{fl})_{SiR}$; [c] see ref.[1a] for the definition of $D_{0.5}$; [d] pulsed STED at 631 nm; [e] CW gated STED at 660 nm (LEICA microsystems); [f] 6′-COOH-X-Rhodamine.

The synthesis of hydroxylated ROX dyes—6′-carboxy derivatives of X-rhodamine (Rhodamine 101), known to have high fluorescence quantum yields both in organic and aqueous solutions—is shown in Scheme 1b. The scrambling condensation between acetate **9** and benzophenone **12a** afforded two other dyes (**13b**,**c**) besides the expected *575RH* (**13a**) due to two consecutive acid-catalyzed reactions: retro-Friedel–Crafts dissociation of **12a** to compounds **10** and **11** (or trimellitic acid), followed by Friedel–Crafts acylation of **9** with **11**. As a result, a new benzophenone with a 2-hydroxy- or 2-acetoxyjulolidine fragment was formed, leading to dihydroxylated dye **13b**. *6-ROX* (**13c**) arose similarly from the retro-Friedel–Crafts byproduct **10**.

The hydroxylated analogues of the unknown bis-(*N*-azetidinyl)-*GeR* and JF_{646}[6]—dyes *630GeRH* and *640SiRH*, respectively—were prepared following the general route on Scheme 2. The method involves a regioselective bromination of di-*O*-TIPS-protected bis(3-hydroxyphenyl)silanes or -germanes **16b**,**c** (TIPS group is required for selectivity) and a double lithium–halogen exchange on dibromides **16** followed by a reaction with dimethylcarbamoyl chloride to yield germa- and silaxanthones **17**. The intermediates **17** are general precursors to the variety of sila- and germafluoresceins and -rhodols, and the proposed approach offers a significant improvement with regard to the number of steps,[6,15] yield[16] and functional group tolerance as compared to earlier preparations.

To evaluate the response of our dyes to the polarity of the media, a series of absorption spectra were recorded in aqueous dioxane solutions with varying water content. The spirolactone–zwitterion equilibrium is shifted in favor of the colored and fluorescent zwitterionic form as the water content increases (Figure 2). For each dye, the $D_{0.5}$ parameter,[1a] an interpolated dielectric constant of the dioxane–water mixture at which the normalized absorption A/A_{max} (or extinction $\varepsilon/\varepsilon_{max}$) of this dye equals one half of the maximal value observed across the entire dioxane–water gradient, was determined (Table 1).

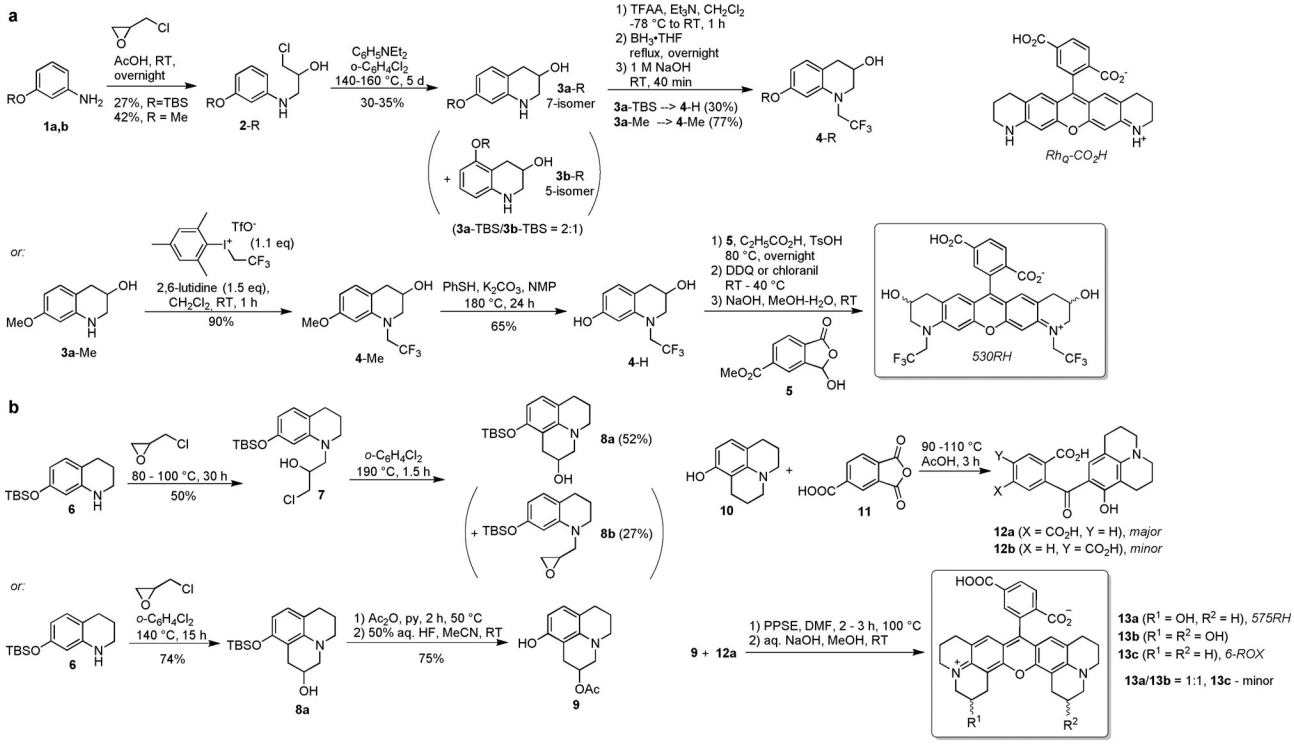

Scheme 1. a) Synthesis of the bis-hydroxylated rhodamine dye *530RH* (an analog of Rh_Q-CO_2H). b) Synthesis of hydroxylated ROX dyes (6-COOH-X-Rhodamines) *575RH* (**13 a**) and **13 b**. Alternative schemes indicate better yielding sequences. PPSE = trimethylsilyl polyphosphate.

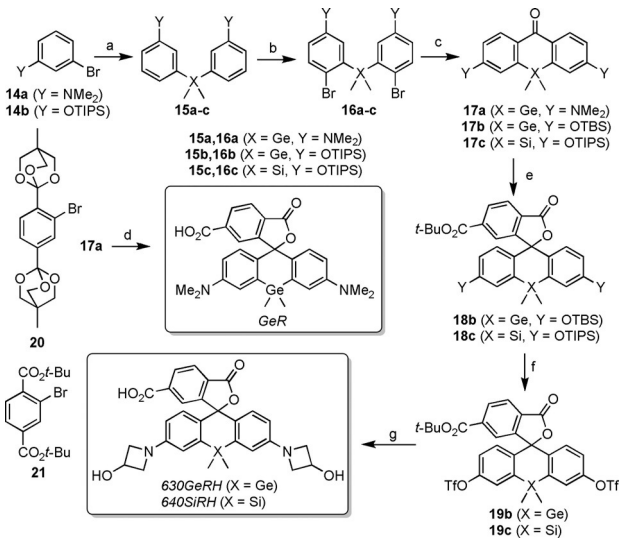

Scheme 2. Synthesis of *GeR* and *SiR* dyes. a) *n*BuLi, −78 °C, then Me_2GeCl_2 or Me_2SiCl_2; b) NBS; c) *n*BuLi or *t*BuLi, −78 °C, then Me_2NCOCl; d) **20**, *t*BuLi (2 equiv), −78 °C to RT, then HCl; e) **21**, *n*BuLi, THF-pentane, −100 °C to RT; f) TBAF, then Tf_2O, pyridine; g) 3-(*tert*-butylsilyloxy)azetidine, cat. $Pd_2(dba)_3$/XPhos, K_2CO_3, dioxane, 100 °C, then TBAF, then TFA.

As expected, the colorless spirolactones of *GeR*, fluorinated rhodamine *530RH* and carbopyronine *560CP* undergo ring opening to the colored and fluorescent zwitterionic forms in systems with high water content, whereas electron-rich *ROX* derivatives remain unresponsive, existing predominantly in the zwitterionic form (Supporting Information Figure S5). Hydroxylation of the *N*-alkyl substituents shifts the position of the equilibrium towards the spirolactone form as can be expected from the weak −*I* effect of β-hydroxy substituents (the increase in $D_{0.5}$ observed upon transition from *SiR* to *640SiRH* and from *GeR* to *630GeRH* is 7–8 units). The hydroxylated dyes display very similar photophysical properties to the parent fluoro-

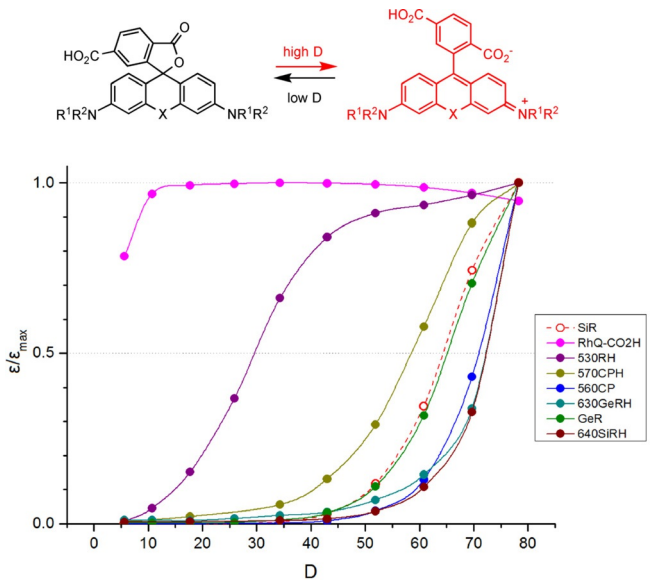

Figure 2. Normalized extinction $\varepsilon/\varepsilon_{max}$ at λ_{max} of the dyes from Table 1 versus dielectric constant *D* of dioxane–water mixtures (*575RH* and *6-ROX* are unresponsive and are not included). The $D_{0.5}$ values correspond to the intersection of interpolated graphs with $\varepsilon/\varepsilon_{max} = 0.5$ line.[1a].

phores, demonstrating up to 0.5 ns longer fluorescence lifetimes and, in the case of *630GeRH*, an improved fluorescence quantum yield.

In agreement with our earlier observations,[1a] HaloTag(O2) amine ligands derived from silico- and germanorhodamines, as well as from fluorinated carbopyronines *560CP* and *570CPH*, demonstrated significant fluorogenic response (increase in fluorescence intensity upon covalent binding to HaloTag protein) in the presence of serum proteins background (Supporting Information Figure S6). The magnitude of the response was consistently smaller for hydroxylated dyes, suggesting a decreased binding affinity of hydroxylated ligands. We can therefore conclude that moderate or high values of $D_{0.5}$ seem to be required, but not sufficient for the desirable fluorogenic behavior of triarylmethane fluorescent labels.[1a,2c]

For the evaluation of performance of our new dyes in super-resolution microscopy, living HeLa and U2OS cells expressing a vimentin-HaloTag fusion protein were incubated for 20 min with 1 μM solutions of *530RH*, *570CPH*, *575RH*, *630GeRH*, as well as non-hydroxylated *GeR* and *6-ROX* (**13c**), conjugated to HaloTag(O2) amine ligand. For labeling of tubulin filaments, HeLa cells were incubated with non-covalent β-tubulin ligands, prepared from *GeR* and *630GeRH* and *N*-Boc-deprotected docetaxel, connected with an 8-aminooctanoic acid linker[2b] (Supporting Information Figure S1). All dye conjugates mentioned above provided specific staining and good imaging performance in confocal and STED microscopy (Supporting Information Figures S7–S17), with hydroxylated dyes generally requiring higher concentrations (e.g., 4–5 μM for *630GeRH* instead of 1 μM or below for *GeR*).

Isomerically pure *6-ROX* dye is one of the "big four" dyes (FAM, JOE, TAMRA and ROX) dominating in the dye-terminator DNA sequencing, but has not yet been applied to live-cell imaging. We have demonstrated that the fluorescence of all *6-ROX* dyes (**13a–c**) may be efficiently switched off by de-excitation at 775 nm, making them useful complementary partners in two-color STED nanoscopy with *SiR* or *GeR* labels. Figures 3, S16 and S17 demonstrate that HaloTag(O2) amine conjugate of *575RH* in combination with *GeR*-tubulin or *630GeRH*-tubulin ligand provide high quality two-color images in the most blue-shifted dye pair still applicable for the widely used 775 nm STED laser line.[17] Comparison of the Figures S9 and S10 confirms that hydroxylation of the rhodamine core in the dye *575RH* improves image quality as related to the commercially available *6-ROX* (Supporting Information Table S1).

In addition to the labeling of cytoskeleton proteins, the new dyes allow for equally specific staining of nuclear components. Living U2OS and *Drosophila* S2 cells expressing SNAP- and Halo-fusion constructs of different nuclear proteins (TRF2, PML, CID, CAL1) were incubated for 10–30 minutes with 0.5–1.0 μM of the chosen dye combination (*610CP*-BG & *640SiRH*-Halo or *580R*-Halo[1a] and *640SiRH*-BG; BG = SNAP-tag ligand) resulting in bright staining free from non-specific background (Supporting Information Figure S18). The excellent spectral separation of these combinations allowed for colocalization experiments without spectral unmixing, mapping the nuclear protein interaction with sub-diffraction resolution (Supporting Information Figure S19).

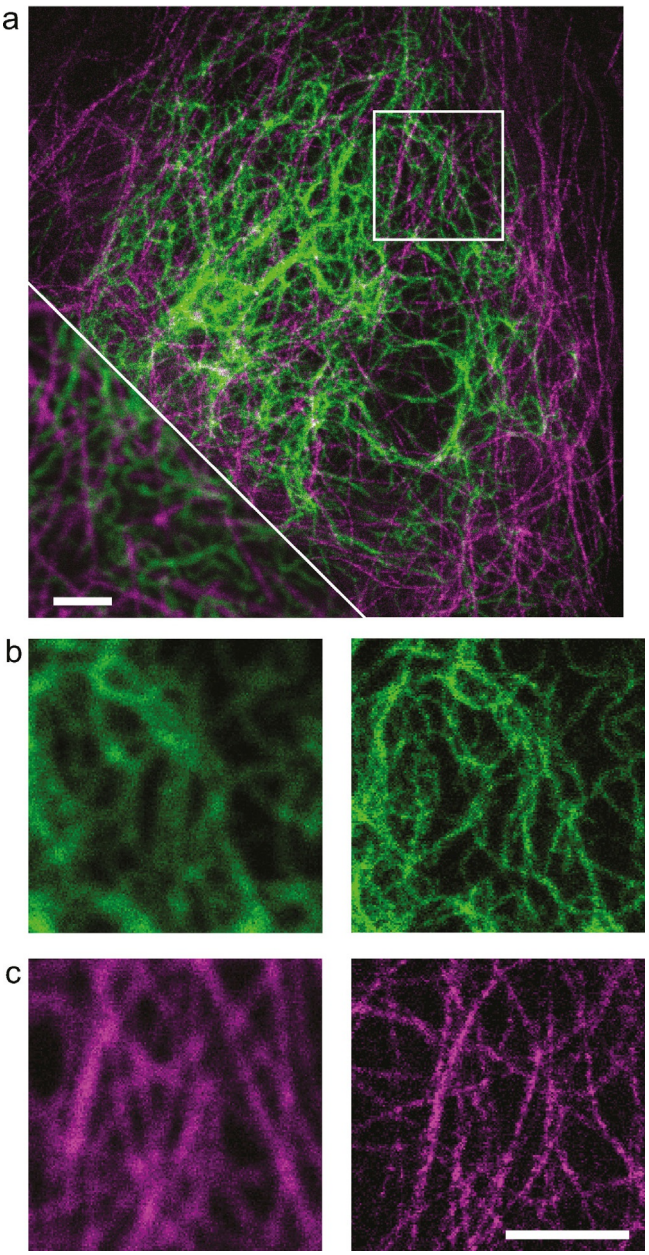

Figure 3. Two-color STED image (raw data) of vimentin-HaloTag fusion protein (green; labeled with 1 μM *575RH*-Halo) and endogeneous tubulin (magenta; labeled with 5 μM *GeR*-tubulin) in living HeLa cells, simultaneous incubation time 20 min, followed by 10 min washing. (a) STED image with confocal part in bottom left corner. (b) and (c): zoomed (confocal and STED) views of the region marked in (a) in separate colors. Scale bars 2 μm; pixel dwell time: 12 μs for both color channels; pixel size: 28 nm for STED and confocal image.

Using so-called holographic microscopy, we have monitored cell morphology and proliferation of living S2 cells with the constant presence of *580R* and *640SiRH* in the media over 12–16 hours and observed normal cell division (Figure 4) with proper staining of the kinetochore proteins, verified with fluorescence microscopy. Therefore, we conclude that the presence

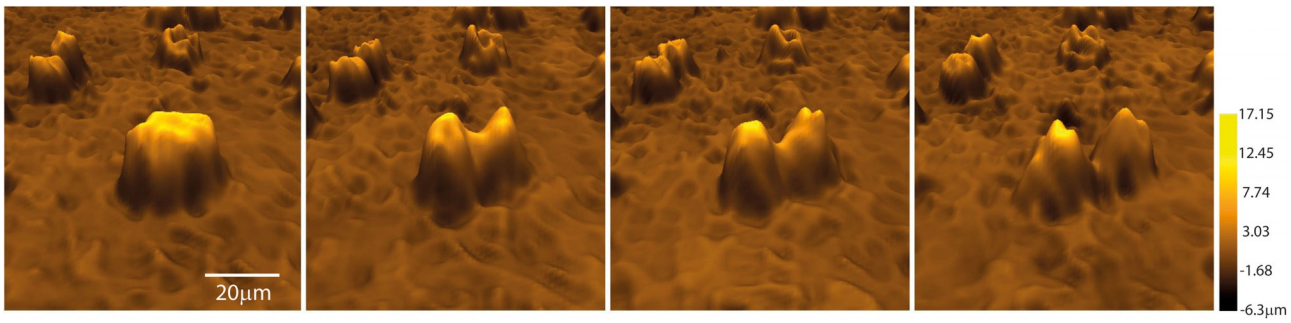

Figure 4. An example of normal cell division (2 min between images) in the presence of *640SiRH* bound to CID-SNAP and *580R* bound to CAL1-Halo after incubation with 0.4 µM *580R*-Halo[1a] (4 h) followed by addition of 0.4 µM *640SiRH*-BG and imaging for 12 h. Cell viability in the presence of dyes in the centromeres was verified by measuring cell morphology of *Drosophila* S2 cells using a holographic microscope (Holomonitor M4). For the corresponding time-lapse movie, see supplementary Movie.

of the protein tags as well as the staining with our dye conjugates does not negatively affect cell viability.

In view of an expanding palette of live-cell compatible dyes and increasing fluorophore substitution diversity, we propose a general method relying on simple additive schemes to estimate the positions of absorption/emission maxima and $D_{0.5}$ values of the substitution pattern analogues of triarylmethane dyes. For example, using the data of our previous study,[1a] the properties of dye *560CP* in the same solvent (PBS, pH 7.4) have been accurately predicted before its synthesis (Scheme 3).

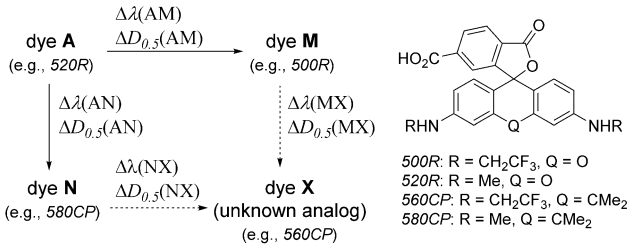

Scheme 3. Three reference dyes (A, M, N) are chosen in such a way that M and N differ from the unknown dye X in one structural element. Dye A has one common structural element with dye M, and another common element with dye N. The known changes in properties between A and M (or N) allow estimation of λ and $D_{0.5}$ for X. Assuming $\Delta\lambda(AN) \approx \Delta\lambda(MX)$ and $\Delta\lambda(AM) \approx \Delta\lambda(NX)$ (in which $\Delta\lambda(AN) = \lambda(N) - \lambda(A)$, valid for both absorption and emission maxima; similarly for $\Delta D_{0.5}$), the estimated values for *560CP* are: $\lambda_{abs}(560CP) = \lambda_{abs}(580CP) + \Delta\lambda_{abs}(520R,500R) = 582 + (500-521)$ nm $= 561$ nm; $D_{0.5}(560CP) = D_{0.5}(580CP) + \Delta D_{0.5}(520R,500R) = 34.6 + (32.5-7.5) = 59.6$. For details, see Figures S20, S21 and Table S2 in the Supporting Information.

In conclusion, the proposed cell- and nucleus-permeant fluorescent dyes allow flexible single- and dual-color labeling in living cells. In STED imaging with de-excitation at 775 nm, several dye pairs have been validated (*575RH* and *635GeRH*, *610CP* and *640SiRH*, and *580R* and *640SiRH*). The improved synthetic approach to silico- and germanorhodamines has been developed, and the new dyes *640SiRH*, *GeR* and *635GeRH* as conjugates with docetaxel offer direct and specific visualization of native tubulin filaments in non-transfected cells. Hydroxylation of fluorophores, especially of lipophilic rhodamines, improves the staining quality at the cost of the necessity to use higher dye loadings. In sub-micromolar concentrations used for imaging, the dyes of the present study show no evidence of cytotoxicity. The design of future dye analogues can be streamlined with accumulation of photophysical data and estimation of properties of the new candidates using simple additive schemes. The degree of predictive precision achieved by using the measured values for the known structural analogues is higher than the accuracy provided by the present-day computational methods (DFT, TD-DFT), especially for the red-emitting fluorophores.[18] Further increasing of the spectral and structural variety of cell-permeant fluorophores will contribute to the design of new experiments in life sciences, including those with more sophisticated multiple color channel separation techniques, such as fluorescence lifetime imaging and hyperspectral detection.

Acknowledgements

We thank J. Bienert (MPIBPC), Dr. H. Frauendorf, Dr. M. John and co-workers (Institut für Organische und Biomolekulare Chemie, Georg-August-Universität, Göttingen, Germany) for recording spectra; Prof. Z. Novák (Eötvös University, Budapest, Hungary) for the gift of trifluoroethyliodonium salt; J. Schimpfhauser and J. Seikowski (MPIBPC) for assistance with the synthesis; Dr. E. Rothermel and T. Gilat (MPIBPC) for the preparation and immunolabeling of cells; Dr. I. Chung, C. Bauer and PD Dr. K. Rippe (Genome Organization and Function, DKFZ) for the U2OS cells used for the nuclear staining and for cloning the TRF2-SNAP and PMLIII-Halo fusion constructs; Dr. A.-L. Pauleau and Prof. S. Erhardt (Zentrum für Molekulare Biologie der Universität Heidelberg, ZMBH) for the *Drosophila S2* cells stably expressing CID-SNAP and CAL1-Halo fusion proteins; Dr. A. Giske (LEICA Microsystems, Germany) for testing *560CP* dye with 660 nm STED laser. S.W.H., A.N.B. and H.S. acknowledge a grant from the Bundesministerium für Bildung und Forschung (FKZ 13N14122). This work was also supported by the Netherlands Organisation for Scientific Research (NWO; grant number 680-50-1501 to R.V.) and EMBO (grant number ALTF 1516–2015 to R.V.).

Conflict of interest

The authors declare no conflict of interest.

Keywords: dyes/pigments · fluorescence · living cells · optical microscopy · rhodamines

[1] a) A. N. Butkevich, G. Y. Mitronova, S. C. Sidenstein, J. L. Klocke, D. Kamin, D. N. Meineke, E. D'Este, P. T. Kraemer, J. G. Danzl, V. N. Belov, S. W. Hell, *Angew. Chem. Int. Ed.* **2016**, *55*, 3290 – 3294; *Angew. Chem.* **2016**, *128*, 3350 – 3355; b) F. Bottanelli, E. B. Kromann, E. S. Allgeyer, R. S. Erdmann, S. Wood Baguley, G. Sirinakis, A. Schepartz, D. Baddeley, D. K. Toomre, J. E. Rothman, J. Bewersdorf, *Nat. Commun.* **2016**, *7*, 10778; c) B. Hein, K. I. Willig, C. A. Wurm, V. Westphal, S. Jakobs, S. W. Hell, *Biophys. J.* **2010**, *98*, 158 – 163; d) S. C. Sidenstein, E. D'Este, M. J. Bohm, J. G. Danzl, V. N. Belov, S. W. Hell, *Sci. Rep.* **2016**, *6*, 26725.

[2] a) G. Lukinavičius, K. Umezawa, N. Olivier, A. Honigmann, G. Yang, T. Plass, V. Mueller, L. Reymond, I. R. Correa, Jr., Z. G. Luo, C. Schultz, E. A. Lemke, P. Heppenstall, C. Eggeling, S. Manley, K. Johnsson, *Nat. Chem.* **2013**, *5*, 132 – 139; b) G. Lukinavičius, L. Reymond, E. D'Este, A. Masharina, F. Gottfert, H. Ta, A. Guther, M. Fournier, S. Rizzo, H. Waldmann, C. Blaukopf, C. Sommer, D. W. Gerlich, H. D. Arndt, S. W. Hell, K. Johnsson, *Nat. Methods* **2014**, *11*, 731 – 733; c) G. Lukinavičius, L. Reymond, K. Umezawa, O. Sallin, E. D'Este, F. Gottfert, H. Ta, S. W. Hell, Y. Urano, K. Johnsson, *J. Am. Chem. Soc.* **2016**, *138*, 9365 – 9368; d) Y. Kushida, T. Nagano, K. Hanaoka, *Analyst* **2015**, *140*, 685 – 695.

[3] L. C. Zanetti-Domingues, C. J. Tynan, D. J. Rolfe, D. T. Clarke, M. Martin-Fernandez, *PLoS One* **2013**, *8*, e74200.

[4] a) Z. Qian, A. Martyna, R. L. Hard, J. Wang, G. Appiah-Kubi, C. Coss, M. A. Phelps, J. S. Rossman, D. Pei, *Biochemistry* **2016**, *55*, 2601 – 2612; b) J. P. Richard, K. Melikov, E. Vives, C. Ramos, B. Verbeure, M. J. Gait, L. V. Chernomordik, B. Lebleu, *J. Biol. Chem.* **2002**, *278*, 585 – 590; c) M. Silhol, M. Tyagi, M. Giacca, B. Lebleu, E. Vives, *Eur. J. Biochem.* **2002**, *269*, 494 – 501.

[5] K. W. Teng, Y. Ishitsuka, P. Ren, Y. Youn, X. Deng, P. Ge, A. S. Belmont, P. R. Selvin, *eLife* **2016**, e20378.

[6] J. B. Grimm, B. P. English, J. Chen, J. P. Slaughter, Z. Zhang, A. Revyakin, R. Patel, J. J. Macklin, D. Normanno, R. H. Singer, T. Lionnet, L. D. Lavis, *Nat. Methods* **2015**, *12*, 244 – 250.

[7] M. J. Hinner, K. Johnsson, *Curr. Opin. Biotechnol.* **2010**, *21*, 766 – 776.

[8] A. Gautier, A. Juillerat, C. Heinis, I. R. Correa, Jr., M. Kindermann, F. Beaufils, K. Johnsson, *Chem. Biol.* **2008**, *15*, 128 – 136.

[9] G. V. Los, L. P. Encell, M. G. McDougall, D. D. Hartzell, N. Karassina, C. Zimprich, M. G. Wood, R. Learish, R. F. Ohana, M. Urh, D. Simpson, J. Mendez, K. Zimmerman, P. Otto, G. Vidugiris, J. Zhu, A. Darzins, D. H. Klaubert, R. F. Bulleit, K. V. Wood, *ACS Chem. Biol.* **2008**, *3*, 373 – 382.

[10] J. Hanne, F. Gottfert, J. Schimer, M. Anders-Osswein, J. Konvalinka, J. Engelhardt, B. Muller, S. W. Hell, H. G. Krausslich, *ACS Nano* **2016**, *10*, 8215 – 8222.

[11] S. Nizamov, M. V. Sednev, M. L. Bossi, E. Hebisch, H. Frauendorf, S. E. Lehnart, V. N. Belov, S. W. Hell, *Chem. Eur. J.* **2016**, *22*, 11631 – 11642.

[12] Y. Koide, Y. Urano, K. Hanaoka, T. Terai, T. Nagano, *ACS Chem. Biol.* **2011**, *6*, 600 – 608.

[13] For structures of the known Ge-rhodamine and Ge-xanthene dyes, see Figure S3 in *Supporting Information* and patents: a) T. Nagano, K. Hanaoka, Y. Koide, T. Egawa, US 20140057312A1; b) J. Braddock-Wilking, T. L. Bandrowski, J. B. Carroll II, US 20150166581; c) T. Nagano, K. Hanaoka, K. Hirabayashi, Y. Yoki, US 20150212073A1; d) W. Zhou, P. Mesenheimer, M. Zhou, US 20140272990A1.

[14] V. P. Boyarskiy, V. N. Belov, R. Medda, B. Hein, M. Bossi, S. W. Hell, *Chem. Eur. J.* **2008**, *14*, 1784 – 1792.

[15] a) T. Egawa, K. Hirabayashi, Y. Koide, C. Kobayashi, N. Takahashi, T. Mineno, T. Terai, T. Ueno, T. Komatsu, Y. Ikegaya, N. Matsuki, T. Nagano, K. Hanaoka, *Angew. Chem. Int. Ed.* **2013**, *52*, 3874 – 3877; *Angew. Chem.* **2013**, *125*, 3966 – 3969; b) T. Egawa, Y. Koide, K. Hanaoka, T. Komatsu, T. Terai, T. Nagano, *Chem. Commun.* **2011**, *47*, 4162 – 4164; c) K. Hirabayashi, K. Hanaoka, T. Takayanagi, Y. Toki, T. Egawa, M. Kamiya, T. Komatsu, T. Ueno, T. Terai, K. Yoshida, M. Uchiyama, T. Nagano, Y. Urano, *Anal. Chem.* **2015**, *87*, 9061 – 9069.

[16] Q. A. Best, N. Sattenapally, D. J. Dyer, C. N. Scott, M. E. McCarroll, *J. Am. Chem. Soc.* **2013**, *135*, 13365 – 13370.

[17] Abberior Instruments GmbH offers STED microscopes with the pulsed 595 nm and 775 nm depletion lasers; Leica Microsystems–with 592 nm (gated; CW), 660 nm (gated; CW) and 775 nm (pulsed) depletion lasers; PicoQuant GmbH offers a STED microscope with a 765 nm depletion laser.

[18] S. Fleming, A. Mills, T. Tuttle, *Beilstein J. Org. Chem.* **2011**, *7*, 432 – 441.

Manuscript received: March 17, 2017
Accepted manuscript online: March 29, 2017
Version of record online: May 2, 2017

